Journal of Nuclear Materials 379 (2008) 97–104

Contents lists available at ScienceDirect

Journal of Nuclear Materials

journal homepage: www.elsevier.com/locate/jnucmat

The effect of radiation on the anaerobic corrosion of steel

N.R. Smart [a,*], A.P. Rance [a], L.O. Werme [b]

[a] Serco Technical and Assurance Services, Culham Science Centre, Abingdon, Oxfordshire OX14 3ED, United Kingdom
[b] Svensk Kärnbränslehantering AB (SKB), Box 5864, SE-10248 Stockholm, Sweden

ARTICLE INFO

PACS:
82.45.Bb
61.82.Bg
61.80.Ed
28.41.Kw

ABSTRACT

To ensure the safe encapsulation of spent nuclear fuel elements for geological disposal, SKB of Sweden are considering using a canister, which consists of an outer copper canister and a cast iron insert. Previous work has investigated the rate of gas generation due to the anaerobic corrosion of ferrous materials over a range of conditions. This paper examines the effect of radiation on the corrosion of steel in repository environments. Tests were carried out at two temperatures (30 °C and 50 °C), two dose rates (11 Gray h^{-1} and 300 Gray h^{-1}) and in two different artificial groundwaters, for exposure periods of several months. Radiation was found to enhance the corrosion rate at both dose rates but the greatest enhancement occurred at the higher dose rate. The corrosion products were predominantly magnetite, with some indications of unidentified higher oxidation state corrosion products being formed at the higher dose rates.

1. Introduction

To ensure the safe encapsulation of spent nuclear fuel elements for geological disposal, SKB (Swedish Nuclear Fuel and Waste Management Co.) of Sweden are considering using the Advanced Cold Process Canister (ACPC), which consists of an outer copper canister and a cast iron insert. A programme of work has been carried out to investigate a range of corrosion issues associated with the canister, including measurements of hydrogen generation due to the anaerobic corrosion of ferrous materials (carbon steel and cast iron) over a range of conditions [1–8]. To date, all this work has been conducted in the absence of a radiation field. Further experiments have been carried out to investigate the rate of gas generation in the presence of representative radiation fields and to analyse the composition of the corrosion product formed, to determine whether radiation has an effect on anaerobic corrosion behaviour [9].

2. Experimental

2.1. Test environments and materials

The measurements were carried out using gas cells of the design used in previous work [7]. Four different environments were examined. These conditions were chosen so that comparison could be made with gas generation rate data obtained previously in the absence of radiation. The four conditions were:

- Modified Allard groundwater 300 Gray h^{-1} at 30 °C.
- Bentonite equilibrated groundwater 300 Gray h^{-1} at 50 °C.
- Modified Allard groundwater 11 Gray h^{-1} at 30 °C.
- Bentonite equilibrated groundwater 11 Gray h^{-1} at 50 °C.

The dose rates given above are representative of the radiation fluxes expected to impinge on the inner and outer surfaces of the cast iron insert in the ACPC, respectively.

The solutions for the experiments were prepared from analytical grade reagents and demineralised water, according to recipes and preparation procedures provided by SKB. The composition of the artificial groundwaters is shown in Table 1.

Cold drawn carbon steel wires with the same composition as used previously were used. They were 1 mm diameter and the total exposed surface area was 0.1 m^2. The composition of the wires was as follows (wt%): C 0.21; Si 0.22; Mn 0.70; P 0.017; S 0.017; Fe bal. To minimise the amount of surface oxide present at the start of the experiments, the metal samples were pickled in inhibited hydrochloric acid, then thoroughly washed, before placing them in the test environment.

2.2. Experimental procedure

The rate of hydrogen production due to the anaerobic corrosion of steel wires in artificial groundwaters under irradiation was measured using a barometric gas cell technique of a design used previously [1–4] (Fig. 1). The cell consisted of two compartments; the first compartment, containing the test specimens, was connected via a gas line to the second compartment, which was a reservoir for a low vapour pressure liquid, di-butyl phthalate (dbp). The second compartment was equipped with a glass manometer column.

* Corresponding author. Tel.: +44 1635 280 385; fax: +44 1635 280 389.
E-mail address: nick.smart@serco.com (N.R. Smart).

0022-3115/$ - see front matter © 2008 Elsevier B.V. All rights reserved.
doi:10.1016/j.jnucmat.2008.06.007

Table 1
Composition of artificial groundwaters used for corrosion experiments

Ion	Bentonite-equilibrated water		Allard water for radiation experiments[c]		Allard water for previous measurements [7]	
	mM	ppm	mM	ppm	mM	ppm
Na^+	560	12880	2.3	52.5	2.84	65.3
Ca^{2+}			0.13	5.1	0.45	18.0
Mg^{2+}			0.03	0.7	0.18	4.4
K^+			0.10	3.9	0.10	3.9
Cl^-	540	19170	1.4	48.8	1.96	69.5
HCO_3^-			1.1	65.0		
CO_3^{2-}	10	600			2.00[b]	120.0
SO_4^{2-}			0.10	9.6	0.1	9.6
SiO_2			0.03	1.7	0.21	12.6
pH[a]	10.4		8.8		8.1	

[a] pH was adjusted by addition of NaOH or HCl as necessary.
[b] Total carbonate.
[c] Prepared in nitrogen-purged glovebox.

Any gas produced by the test pieces caused a pressure increase, which reduced the level of dbp in the reservoir and increased the level in the manometer tube. By measuring the height of the liquid in the manometer tube and the volume of dbp displaced by expanding gas it was possible to calculate the volume of hydrogen produced by anaerobic corrosion. The results were corrected for the external atmospheric pressure. The volume of liquid in the test cells was ~150 ml.

It was thought probable that exposure of the gas cells and the water in them to radiation would result in some gas release due to radiolytic breakdown of the materials of construction and for this reason it was necessary to set up a control cell for each test environment. To minimise the gas release due to radiation, the test solutions and samples were placed in zirconia crucibles, rather than the polyethylene vessels used previously, as polyethylene was likely to suffer from radiolytic degradation. Zirconia was chosen rather than alumina because it is less susceptible to alkaline attack. The four control cells were identical to the four test cells, but did not contain any steel wires. The control cells were used to monitor the amount of gas produced by radiolytic degradation of the materials.

The cells were prepared by posting all the cell components into a nitrogen-purged glovebox, with the exception of the precision bore manometer tube, which was too large to fit into the glovebox, but including the freshly pickled wires. This procedure was to ensure that the residual oxygen concentration in the nitrogen cover gas at the start of the experiments was minimised. The test solutions were prepared inside the glovebox. After adding the deaerated test solution to the crucible containing the test wires, the cell was assembled by joining the ground glass joints of the gas cell using two-part epoxy resin (Araldite MY753 HY951 hardener). When the epoxy resin had cured, the cells were sealed by closing the tap above the dbp reservoir and removed from the glovebox. The manometer tube was then attached and the cells were then ready to be inserted in to the radiation cell.

After assembly, each pair of cells (i.e. one test cell plus one control cell) was maintained at the required test temperature by placing them in ovens, which had openings in the top to accommodate the manometers. Lagging was placed around the exit hole for the manometers. The temperature in each of the ovens was controlled

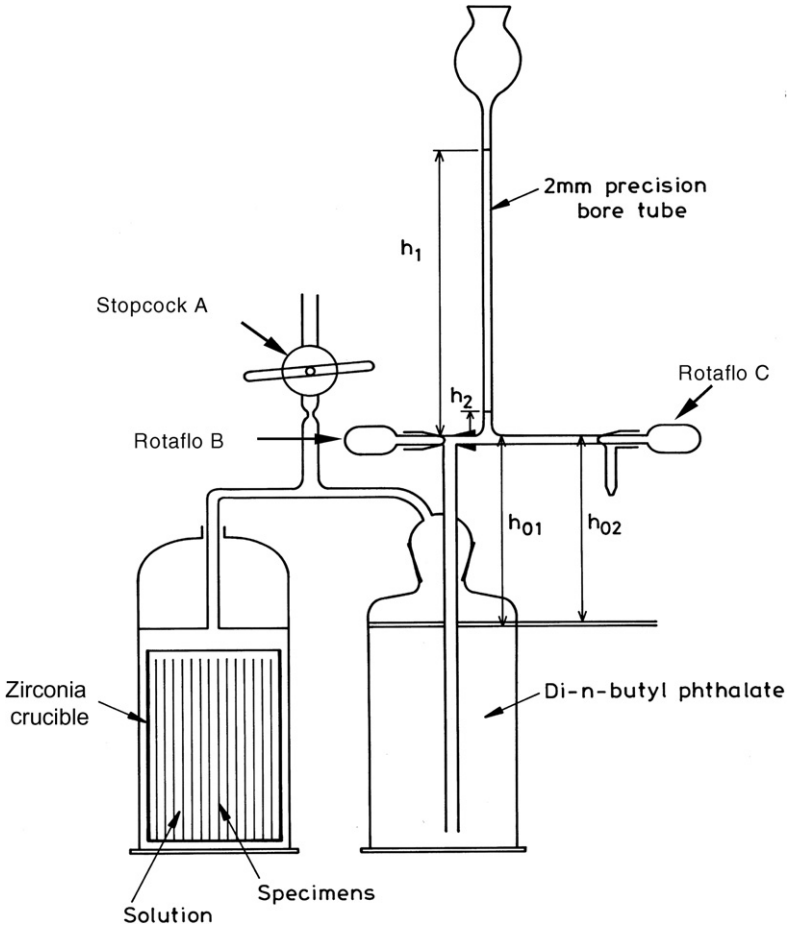

Fig. 1. Diagram of gas cell used to measure hydrogen production due to anaerobic corrosion of carbon steel under irradiated conditions.

using a Eurotherm temperature controller and type K thermocouple. The required γ-radiation dose rates were achieved by placing the ovens at appropriate distances from the cobalt-60 source (average energy 1.25 MeV) in a gamma irradiation facility at Harwell, Oxfordshire, UK. The dose rates were measured directly using a Farmer dose meter and ion chamber, which were calibrated to national standards.

Gas production measurements were made at appropriate intervals to accommodate the expected initial high rate and the subsequent rate reduction. The procedures for measuring the amount of gas generated and calculating the corresponding corrosion rates are given in [9]. From time to time it was necessary to refill the dbp reservoir as the level was reduced by the evolution of gas. The procedure for doing this is given in [9]. Due to essential refurbishment work on the radiation cell it was necessary to remove some of the gas cells from the radiation test facility cell for a few weeks during the course of the experiments.

2.3. Analysis of samples

At the end of the experiments the cells were dismantled and the pH values of the solutions were measured. Photographs were taken to show the condition of the test specimens at the end of the exposure period. One wire from each cell was analysed by Raman spectroscopy to determine the composition of the corrosion product. The cells were dismantled in a nitrogen-purged glove box and single wires, which were still wetted by the test solution, were sealed in capillary tubes to ensure that they were not exposed to air. The capillary tubes were sealed with a blob of epoxy resin, which was allowed to harden. The tubes were then removed from the glovebox and the glass was sealed by rapidly fusing it in a gas flame at a point well away from the sample so that the latter was not heated significantly. The sample was then transferred to the Raman spectrometer for analysis.

A Renishaw Laser Raman Microprobe was used to analyse the surface of the corroded wires through the glass walls of the capillary tubes. The exciting laser wavelength of 688 nm was obtained using a red HeNe laser, capable of delivering up to 100 mW total power, measured at the output from the laser. The detector was a peltier-cooled CCD array. The laser was coupled to the sample via a 180° backscattered arrangement using a Leitz optical microscope with high numerical aperture objective lenses (20× and 50× magnification). The Rayleigh scattered light was removed via a notch filter and the Raman scattered light dispersed via holographic diffraction gratings. The spectrometer was capable of recording over a wide wavenumbers shift range, but spectra were recorded over a limited range of ca. 200–800 cm^{-1}, which covered the main bands expected from iron corrosion products.

3. Results

3.1. Measurements in Allard groundwater

The gas evolution rates from the control cells are shown in Fig. 2. The results of the gas generation experiments in Allard water at two radiation levels at 30 °C are shown in Figs. 3 and 4. The corrosion rate data are based on the assumption that the final corrosion product was magnetite (Fe_3O_4), formed by the overall reaction:

$$3Fe + 4H_2O \rightarrow Fe_3O_4 + 4H_2 \uparrow \quad (1)$$

For comparison, the data obtained for carbon steel in unirradiated Allard water at 30 °C are also given in Figs. 3 and 4; the data for unirradiated conditions were taken from earlier studies [3,5,7]. The Allard water used for the unirradiated tests had a slightly different composition to that used for the irradiated tests, as shown in Table 1.

3.2. Measurements in bentonite-equilibrated groundwater

The results of the gas generation experiments in bentonite-equilibrated groundwater at two radiation levels at 50 °C are shown in Fig. 5–7. For comparison purposes, the data for carbon steel in unirradiated bentonite-equilibrated groundwater at 50 °C [4] are also shown.

3.3. Analysis of corrosion product

The samples tested at the low dose rate were black and the solution was clear, whereas the solution tested at the high dose rate had a milky appearance and the corrosion product had a slight brown tinge to it [9]. It was also found that there was a layer of dark brown sludge at the bottom of the test cell.

Multiple Raman spectra were recorded from each of the samples and a representative spectrum from each is shown in Figs. 8–10. All three wire samples displayed a strong Raman band at

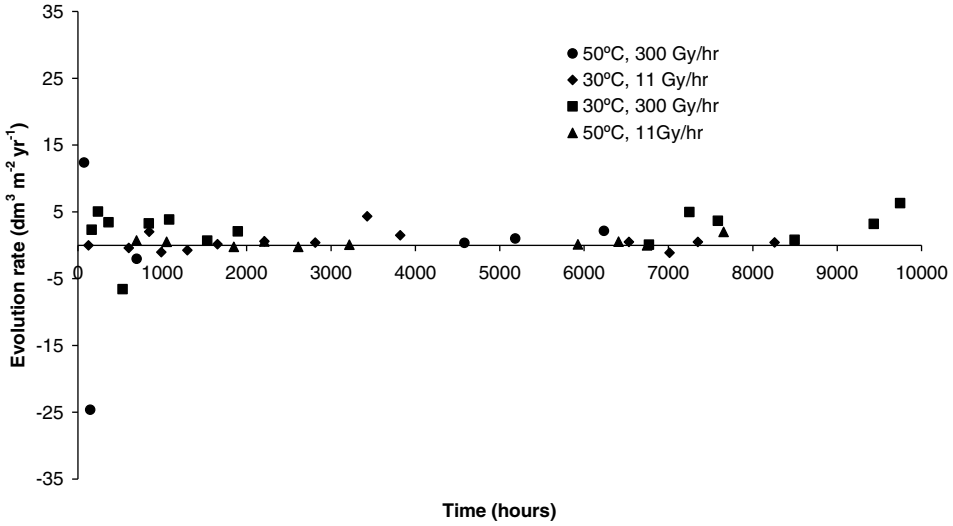

Fig. 2. Gas evolution rate from dummy cells.

ca. 660 cm^{-1} and this is indicative of magnetite. For comparison, the reference spectrum of magnetite is overlaid on these spectra [10]. Other phases of oxidised iron, in particular the oxyhydroxides, may also have been present, although no definitive attribution could be made from the data. For comparison, Table 2 lists the peak positions of three different FeOOH phases [11]. There were no indications of iron carbonate, or green rusts, a series of Fe(II)–Fe(III) compounds, for which a characteristic peak at 430 cm^{-1} would be expected [12].

The pH of the test solution in the cells containing the wires was measured after dismantling and the results are shown in Table 3.

4. Discussion

Tests have been carried out to measure the anaerobic corrosion rates of steel and the corresponding hydrogen generation rates under radiation levels simulating those on the inner and outer surfaces of the cast iron insert, using two simulated groundwaters, two test temperatures and two radiation levels. Some gas generation was measured from the dummy cells (Fig. 2) but it was considerably less than that measured for the test cells containing wires. The gas generation rate in the dummy cells appeared to be highest at the highest radiation dose, presumably due to radiolytic breakdown of the cell components or contents.

At 30 °C and a dose rate of 11 Gray h^{-1}, the corrosion rate in Allard water was higher than in unirradiated conditions (Fig. 3) by a factor of about 6 initially, but after 7000 h the corrosion rate was similar to the corrosion rate for unirradiated conditions, suggesting that once the corrosion product film had become fully developed the effect of radiation was negligible. At the same temperature, but at a dose rate of 300 Gray h^{-1} (Fig. 4), the initial corrosion rate was also higher than in unirradiated conditions, but the increase in corrosion rate was maintained over the entire test period. This test was interrupted, because it was necessary to remove the cell from the radiation cell during the course of the experiment for essential maintenance, but when the cell was re-exposed to the radiation source, there was an increase in gas generation. This supports the view that the presence of radiation increased the corrosion

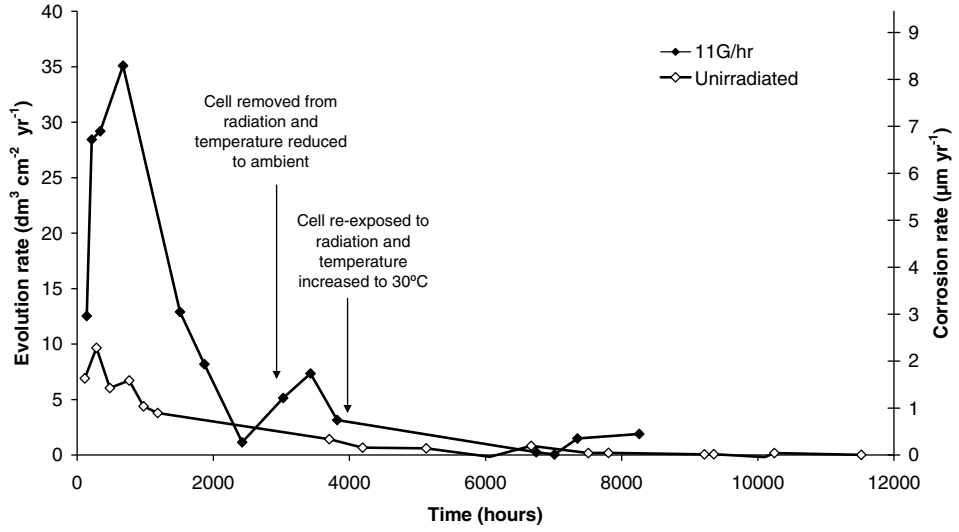

Fig. 3. Hydrogen evolution rates and corrosion rates for carbon steel in anoxic Allard water at 30 °C and 0 Gray h^{-1} and 11 Gray h^{-1} (see Table 1 for composition of Allard waters).

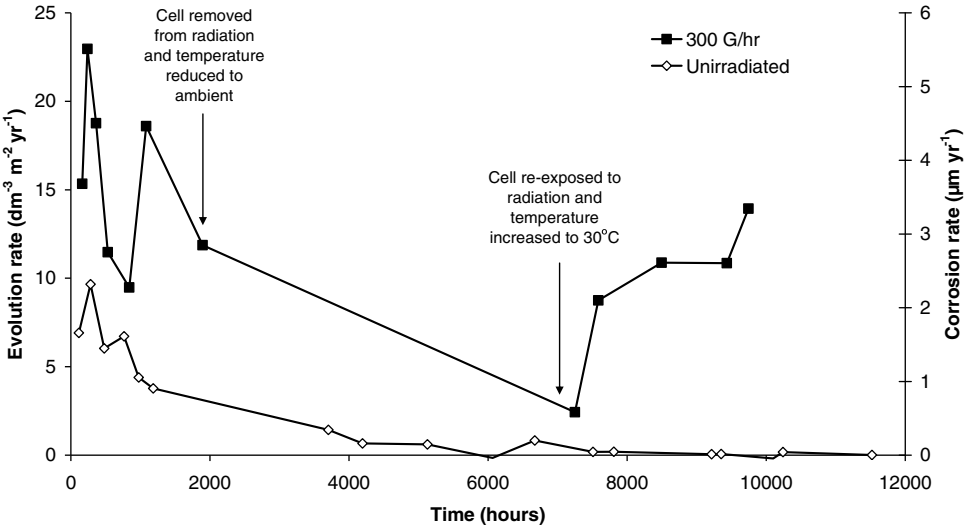

Fig. 4. Hydrogen evolution rates and corrosion rates for carbon steel in anoxic Allard water at 30 °C and 0 Gray h^{-1} and 300 Gray h^{-1} (see Table 1 for composition of Allard waters).

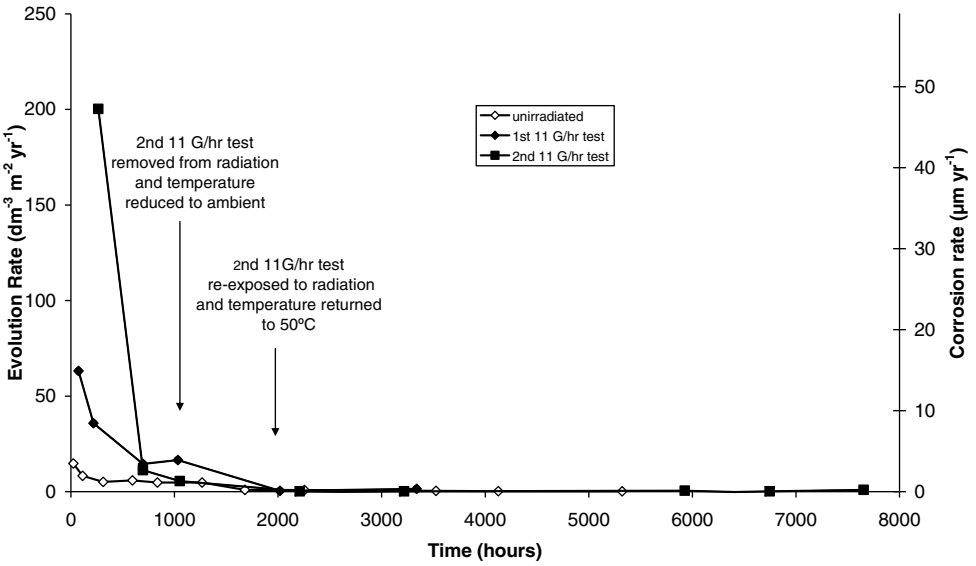

Fig. 5. Hydrogen evolution rates and corrosion rates for carbon steel in anoxic bentonite-equilibrated groundwater at 50 °C at 0 Gray h^{-1} and 11 Gray h^{-1}.

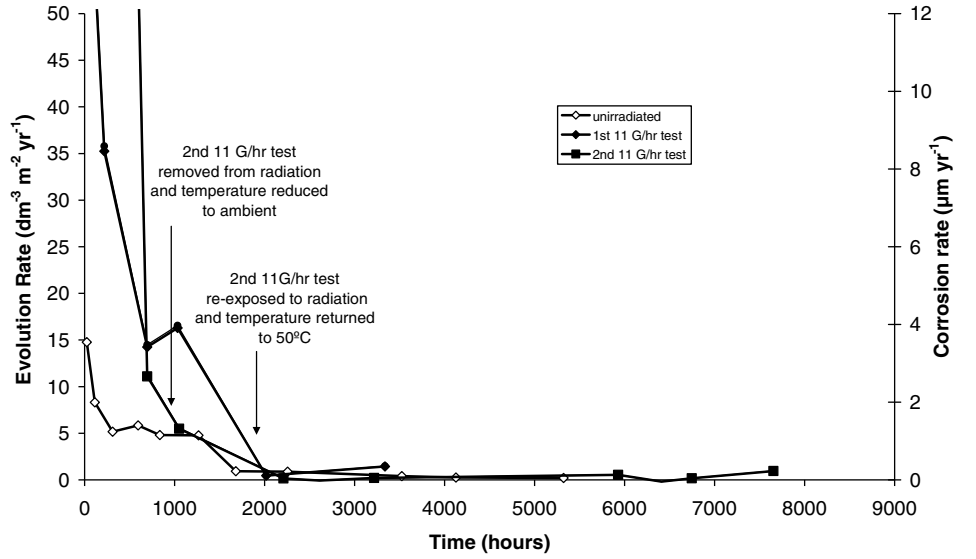

Fig. 6. Hydrogen evolution rates and corrosion rates for carbon steel in anoxic bentonite-equilibrated groundwater at 50 °C at 0 Gray h^{-1} and 11 Gray h^{-1} – expanded scale.

rate. The final reading on the test cells gave a corrosion rate value of ~3 μm $year^{-1}$, compared to <0.1 μm $year^{-1}$ without radiation.

At 50 °C and 11 Gray h^{-1}, both tests in bentonite-equilibrated groundwater gave a higher corrosion rate initially compared to the results obtained previously under unirradiated conditions (Fig. 5). However after ~2000 h, the corrosion rate was very similar to that measured in the absence of radiation (Fig. 6), and after ~4000 h the corrosion rate for both irradiated and unirradiated conditions was ~0.05–0.2 μm $year^{-1}$. At the higher dose rate (i.e. 300 Gray h^{-1}), the corrosion rate remained higher throughout the test (Fig. 7), and after 5000 h the corrosion rate was ~0.8 μm $year^{-1}$ compared to 0.05 μm $year^{-1}$ without radiation. Approximately 25% of this apparent increase in corrosion rate at 5000 h was probably attributable to gas production from other materials within the cell apart from the steel, as shown by the dummy cell results (Fig. 2). Nevertheless there appears to be a real increase in corrosion rate as a result of the high radiation dose.

For comparison, Marsh and Taylor [13] carried out corrosion experiments on 0.2% carbon forged steel in argon-purged synthetic groundwater (pH 9.4), with and without radiation. The ionic strength and pH of the artificial groundwater used in their work were similar to the Allard water used in the present tests (Table 1). On the basis of weight loss measurements, Marsh et al. found that the integrated corrosion rate after 5000 h in unirradiated conditions was ~0.1 μm $year^{-1}$, with no localised attack. In the same environment with a radiation dose of 1000 Gray h^{-1}, the corrosion rate was constant at ~3 μm $year^{-1}$, for test periods of up to 5236 h, with no localised attack developing. These corrosion rates are similar to those measured in the current work in the Allard water, as shown in Fig. 4. No localised attack was observed in the current tests either. The fact that similar corrosion rates have been observed on the basis of weight loss and hydrogen generation measurements suggests that the increased volume of hydrogen produced is a result of corrosion, rather than radiolysis processes in the test cell.

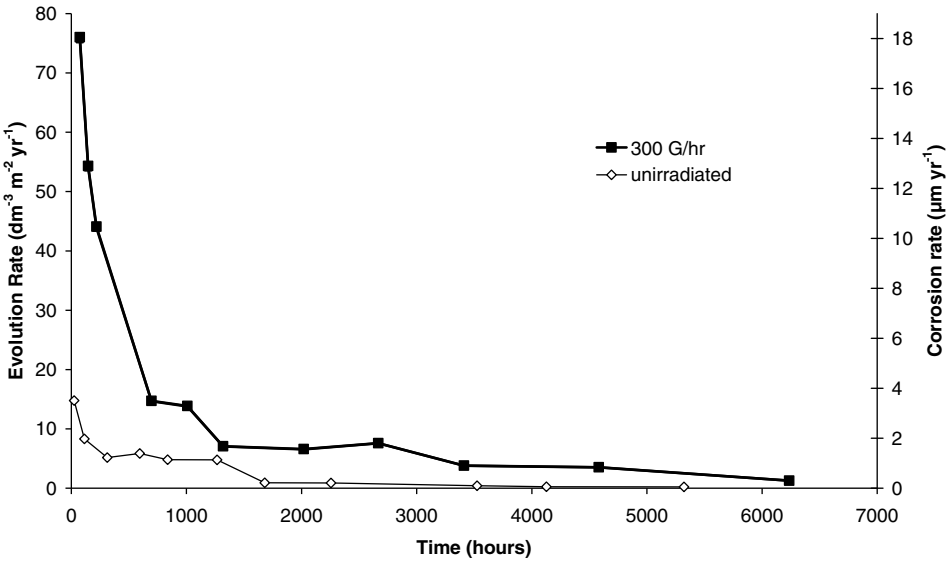

Fig. 7. Hydrogen evolution rates and corrosion rates for carbon steel in anoxic bentonite-equilibrated groundwater at 50 °C at 0 Gray h^{-1} and 300 Gray h^{-1}.

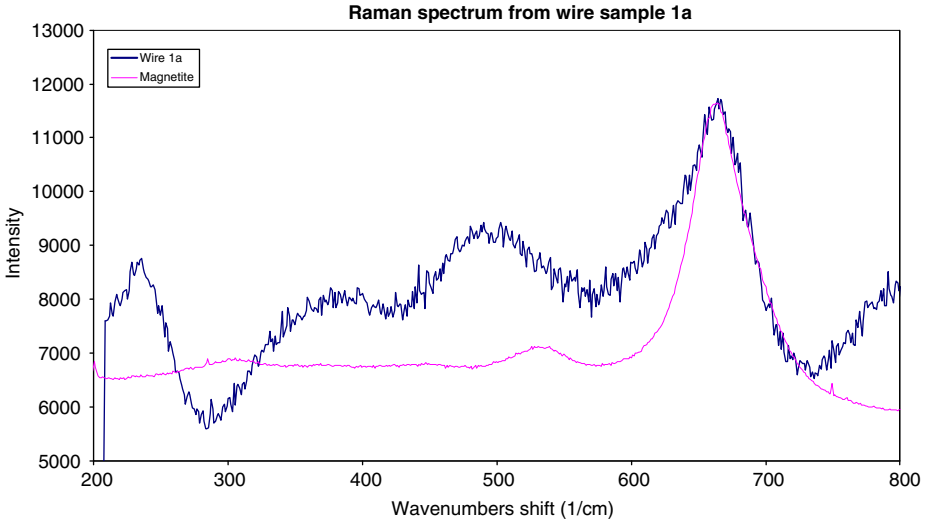

Fig. 8. Raman spectrum for corrosion product formed on carbon steel wire in anoxic bentonite-equilibrated groundwater at 50 °C and 11 Gray h^{-1}.

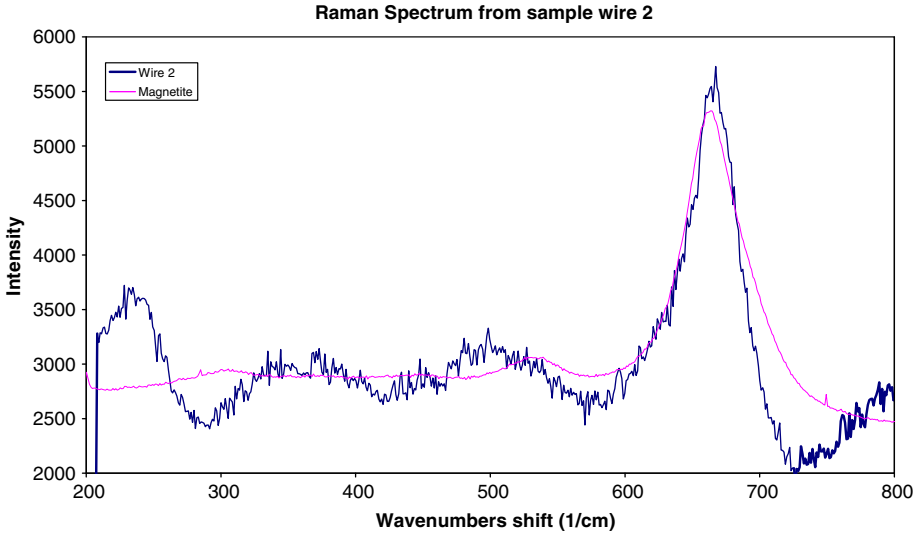

Fig. 9. Raman spectrum for corrosion product formed on carbon steel wire in anoxic bentonite-equilibrated groundwater at 50 °C and 300 Gray h^{-1}.

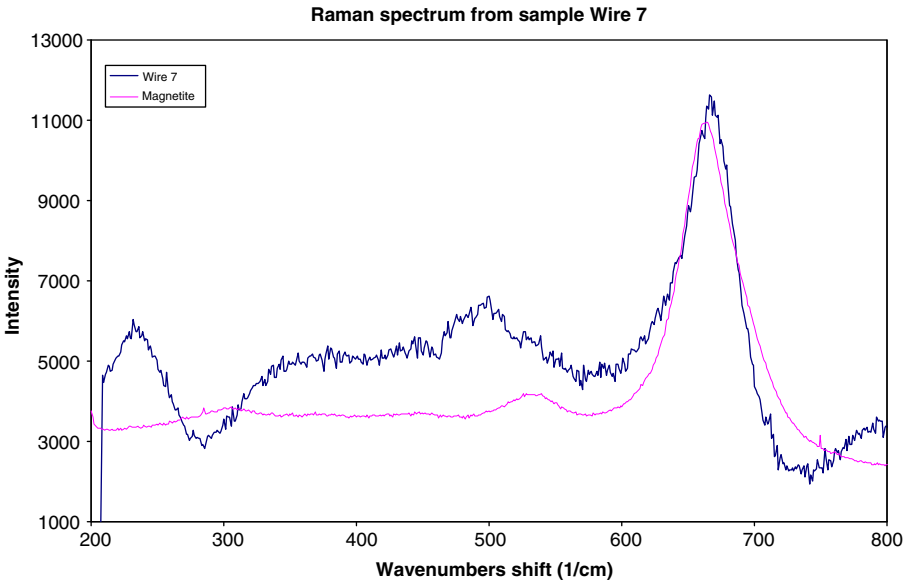

Fig. 10. Raman spectrum for corrosion product formed on carbon steel wire in anoxic Allard groundwater at 30 °C and 11 Gray h^{-1}.

Table 2
Raman peak positions of FeOOH phases

Mineral	Formula	Peak positions
Goethite	α-FeOOH	243, 299, 385 (main), 479, 550
Lepidocrocite	γ-FeOOH	245 (main), 373, 522 (minor)
–	δ-FeOOH	400 (very broad), 680 (broad)

Table 3
pH of test solutions containing wires at end of gas measurement experiments

Cell number	Environment	pH at end of test
5	Allard groundwater 300 Gray h^{-1}@ 30 °C	Not dismantled
2	Bentonite equilibrated groundwater 300 Gray h^{-1}@ 50 °C	9.07
7	Allard groundwater 11 Gray h^{-1}@ 30 °C	9.30
1a	Bentonite equilibrated groundwater 11 Gray h^{-1}@ 50 °C	8.97

Other workers have reported that the corrosion rates of iron-based alloys under irradiated conditions are generally 2–3 times higher than those obtained on similar materials under non-irradiated conditions at 150 °C [14].

The main corrosion product detected by Raman spectroscopy was magnetite, although there is a possibility that there was also a small amount of FeOOH present. Comparison with Raman spectra acquired for wires that had been corroded in the absence of radiation [15] shows that radiation may lead to the formation of some additional iron oxy-hydroxide species, which showed up as additional peaks in the Raman spectra at lower wavenumbers than the magnetite peak, but it has not been possible to conclusively attribute these peaks to specific species. It was observed that the corrosion product formed under a high dose rate was a different colour to the specimens produced at 0 Gray h^{-1} or 11 Gray h^{-1} – it had a brownish tinge to it, rather than being completely black. There also appeared to be more corrosion product produced, which collected as a sludge at the bottom of the cell. These results suggest that the presence of radiolysis species in the solution leads to the formation of different higher oxidation state iron corrosion products, as well as magnetite, but their exact composition has not been characterised.

When water radiolysis occurs, hydrogen, hydrogen peroxide, hydroxyl radicals, aqueous electrons, oxygen and a number of other reactive species may be formed [16]. However the concentration of the various species will depend on a number of factors [17,18] including the composition of the solution under irradiation [19], the dose rate and the concentration of hydrogen produced by the corrosion reaction. In addition it is possible that the nitrogen used as a cover gas in the test cells may have been consumed in radiolysis reactions, for example to produce nitric acid. To obtain a fuller understanding, more detailed radiochemical modelling of the conditions in the present tests would be required.

5. Conclusions

The main conclusions from this work are as follows:

1. The presence of gamma radiation fields increases the anaerobic corrosion rate of carbon steel in artificial groundwaters simulating those expected in the SKB repository. At 11 Gray h^{-1} the increase only lasts for approximately 7000 h, but at 300 Gray h^{-1} the enhancement is longer lasting and may be continuous.
2. The enhancement in the corrosion rate is greater in Allard water, where a 30 fold increase in corrosion rate was observed, than in bentonite-equilibrated groundwater, which had a higher ionic strength and a higher initial pH, where the radiation-induced enhancement was 10–20 times.
3. The predominant corrosion product of anaerobic corrosion of iron under irradiated conditions is magnetite, but there was some evidence of higher oxidation state oxyhydroxides under the high dose rate conditions.
4. A more detailed analysis of the radiochemical conditions in the tests is required to develop an improved understanding of the reasons for the increase in corrosion rate under irradiation.

Acknowledgements

The authors are grateful to Colin Johnston, Department of Materials, Oxford University, for carrying out the Raman spectroscopy analysis, John Dawson (Serco) for assistance with setting up the experiments in the radiation cell and SKB for financial support.

References

[1] D.J. Blackwood, A.R. Hoch, C.C. Naish, A.P. Rance and S.M. Sharland, Research on Corrosion Aspects of the Advanced Cold Process Canister, AEA-D& W-0684, SKB Technical Report 94–12, 1994.

[2] D.J. Blackwood, C.C.Naish, A.P. Rance, Further Research on Corrosion Aspects of the Advanced Cold Process Canister, AEA-ESD-0052, SKB-PR-95-05, 1994.

[3] D.J. Blackwood, C.C. Naish, N. Platts, K.J. Taylor, M.I. Thomas, The Anaerobic Corrosion of Carbon Steel in Granitic Groundwaters, AEA Technology Report, AEA-InTec-1414, 1995.

[4] N.R Smart, A.P. Rance, D.J. Blackwood, Corrosion Aspects of the Copper–steel/iron Process Canister: Consequences of Changing the Material for the Inner Container from Carbon Steel to Cast Iron, SKB 97–04, 1997.

[5] N.R. Smart, D.J. Blackwood and L. Werme, The Anaerobic Corrosion of Carbon Steel and Cast Iron in Artificial Groundwaters, SKB Report TR-01-22, 2001.

[6] N.R. Smart, D.J. Blackwood, L. Werme, Anaerobic corrosion of carbon steel and cast iron in artificial groundwaters: Part 1-electrochemical aspects, Corrosion 58 (7) (2002) 547.

[7] N.R. Smart, D.J. Blackwood, L. Werme, Anaerobic corrosion of carbon steel and cast iron in artificial groundwaters: Part 2-Gas generation, Corrosion 58 (8) (2002) 627.

[8] N.R. Smart, A.P. Rance, L.O. Werme, Anaerobic Corrosion of Steel in Bentonite, in: V.M. Oversby, L.O. Werme (Eds.), Scientific Basis for Nuclear Waste Management XXVII, Materials Research Society Symposium Proceedings, vol. 807, 2004, p. 441.

[9] N.R. Smart, A.P. Rance, Effect of Radiation on Anaerobic Corrosion of Iron, Serco report SA/EIG/15030/C001, 2004 and SKB report TR-05-05, 2005.

[10] From California Institute of Technology Mineral Database.

[11] D.L.A. de Faria, S. Venâncio Silva, M.T. Oliveira, Raman microspectroscopy of some iron oxides and oxyhydroxides, J. Raman Spectrosc. 28 (1997) 873.

[12] Ph. Refait, J.-B. Memet, C. Bon, R. Sabot, J.M.R. Génin, Formation of the Fe(II)–Fe(III) hydroxysulphate green rust during marine corrosion of steel, Corros. Sci. 45 (2003) 833.

[13] G.P. Marsh, K.J. Taylor, An assessment of carbon steel containers for radioactive waste disposal, Corros. Sci. 28 (1988) 289.

[14] J.L. Nelson, R.E. Westerman, F.S. Gerber, Irradiation-corrosion evaluation of metals for nuclear waste package applications in grande ronde basalt groundwater in scientific basis for nuclear waste management X, in: G.L. McVay (Ed.), Materials Research Society Symposium Proceedings, vol. 26, 1984, p. 121.

[15] A.P. Rance, R. Peat, N.R. Smart, Analysis of SKB Electrochemistry Cells, SA/RJCB/62036/R01, and SKB report TR-04-01, 2003.

[16] Z. Cai, X. Li, Y. Katsumura, O. Urabe, Radiolysis of bicarbonate and carbonate aqueous solutions: product analysis and simulation of radiolytic processes, Nucl. Technol. 136 (2001) 231.

[17] H. Christensen, S. Sunder, An evaluation of water layer thickness effective in the oxidation of UO_2 fuel due to radiolysis of water, J. Nucl. Mater. 238 (1996) 70.

[18] G.V. Buxton, C.L. Greenstock, W.P. Hellman, A.B. Ross, Critical review of rate constants for reactions of hydrated electrons, hydrogen atoms and hydroxyl radicals in aqueous solutions, J. Phys. Chem. Reference Data 17 (1988) 513.

[19] S. Sunder, H. Christensen, Gamma radiolysis of water solutions relevant to the nuclear waste management program, Nucl. Technol. 104 (1993) 403.